NVE

RAPPORT

Nr 48/2019

Reanalysing a glacier mass balance measurement series - Langfjordjøkelen 2008-2018

Bjarne Kjøllmoen

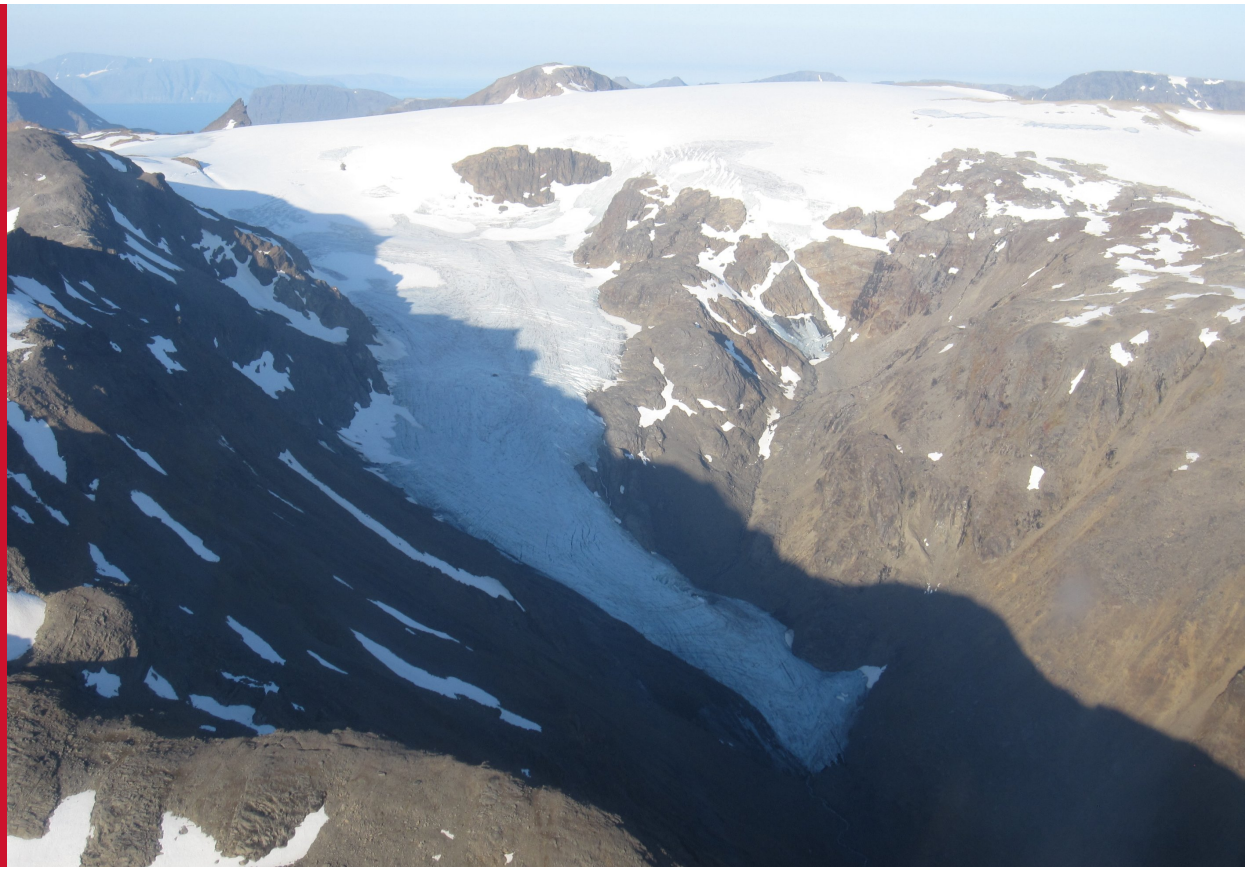

Rapport, engelsk nr 48-2019

Reanalysing a glacier mass balance measurement series - Langfjordjøkelen 2008-2018

Published by: Norges vassdrags- og energidirektorat
Author(s): Bjarne Kjøllmoen

Printing: NVEs hustrykkeri
Forsidefoto: Langfjordjøkelen 29th September 2017. Photo: Bjarne Kjøllmoen
ISBN: 978-82-410-1957-9
ISSN: 1501-2832

Summary: The glaciological mass balance series for Langfjordjøkelen covers the period 1989-2018. In this report, a re-analysed time series is presented.

Keywords: Mass balance, Digital Terrain Models, Re-analysis, Homogenization

Norwegian water resources and energy directorate (NVE)
Middelthunsgate 29
P.O. box 5091 Majorstua
0301 OSLO,
Norway

Telephone: +47 22 95 95 95
Email: nve@nve.no
Internet: www.nve.no

November 2019

Reanalysing a glacier mass balance measurement series – Langfjordjøkelen 2008-2018

Norwegian Water Resources and Energy Directorate
2019

Contents

Preface

This report documents the results from reanalysis of mass balance measurements at Langfjordjøkelen. The time series is based on traditional glaciological observations using stakes and probings, as well as geodetic observations using laser scanning and digital terrain models.

This report is prepared and written by Bjarne Kjøllmoen.

The work is also a contribution to NVE internal project “Massebalanse 80118”.

Oslo, November 2019

Rune Engeset
Head of section

Bjarne Kjøllmoen
Senior engineer

Summary

The glaciological and geodetic methods provide independent observations of glacier mass balance. The glaciological method is based on annual surface mass balance measurements, whereas the geodetic method includes surface measurements, and estimates of internal and basal mass balance over a period of years.

The glaciological mass balance series for Langfjordjøkelen covers the period from 1989 to 2018. Within this period, usable Digital Terrain Models (DTMs) from 1994, 2008 and 2018 were generated. In this report, a re-analysed time series is presented. The re-analysis includes homogenization of both glaciological and geodetic observation series, uncertainty assessment and comparison of the glaciological and geodetic mass balance.

One period of data sets (2009-2018) was compared and the results did not show significant discrepancies between the glaciological and geodetic methods.

The re-analysed glaciological cumulative mass balance over 1989-2018 was −27.5 m w.e., while the original mass balance over the same period was −29.3 m w.e.

1 Introduction

1.1 Background

The Norwegian Water Resources and Energy Directorate (NVE) operate the Norwegian mass balance observation programme. The observations are both traditional field measurements, referred to as the "glaciological method" (also called direct, conventional or traditional method) and geodetic surveys, referred to as the "geodetic method" (Cogley et al., 2011). This report describes the reanalysis of the Langfjordjøkelen time series.

The glaciological mass balance method measures surface mass balance at point locations, and data are extrapolated over the entire glacier surface to obtain glacier-wide averages. The cumulative mass balance is the sum of the annual balances. In the geodetic method, cumulative balance is calculated from glacier surface elevations measured in different years by differencing Digital Terrain Models (DTMs) and by converting the volume change to mass change using a density conversion. The geodetic method is often used as a check on the accuracy of annual measurements by the glaciological method (e.g. Andreassen, 1999 and Zemp, 2010). If a comparison between the glaciological and the geodetic method of a time series show great discrepancies, a calibration of the glaciological mass balance series is required.

1.2 Langfjordjøkelen

Langfjordjøkelen (70°10'N, 21°45'E) is a plateau glacier (Fig. 1) situated in northern Norway, approximately 60 km northwest of the city of Alta. It has an area of 6.3 km^2 (2018) and of this 2.6 km^2 drains eastward. The investigations are performed on this east-facing part ranging from 338 to 1043 m a.s.l. The upper part of the glacier is a small plateau, with an even gently sloping surface down to about 870 m a.s.l. Between 850 and 750 m a.s.l. the glacier flows through a steep icefall. The distance along a central flow line is 4.6 km, from the upper ice divide in north, to the glacier terminus in east.

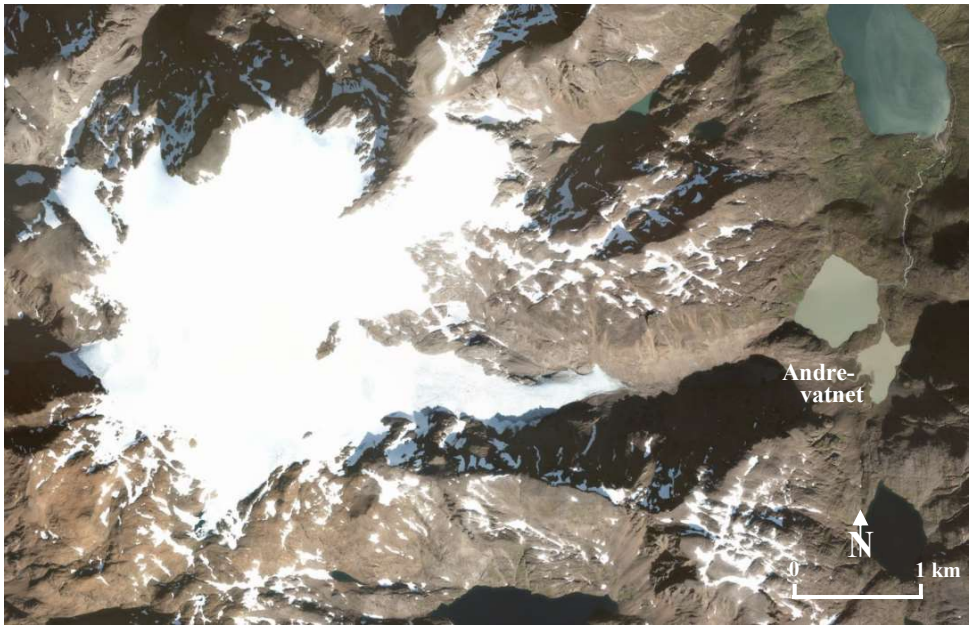

Figure 1
The ice cap Langfjordjøkelen photographed on 21st August 2015. Source: norgeibilder.no.

1.3 Previous results

Langfjordjøkelen has been surveyed by aerial photography in 1966 and 1994, and by laser scanning (LIDAR) in 2008 and 2018. Detailed glacier maps have been constructed from all these mappings.

The east-facing part of Langfjordjøkelen has been subject for annual glaciological mass balance measurements since 1989 (Kjøllmoen et al., 2018). The series are complete with exception of the years 1994 and 1995, which was estimated in Kjøllmoen and Olsen (2002). For the first eight years, from 1989 to 1996, the glacier was near balance (a small deficit), but from 1996 to 2018 the results show a great deficit. The reported original glaciological mass balance showed a deficit of −27.2 m w.e. for the period 1989-2017 included estimated values for 1994 and 1995. A homogenized mass balance series for 1989-1993 and 1996-2009 was presented in Kjøllmoen et al. (2016).

Geodetic mass balance was calculated for the two periods 1966-1994 and 1994-2008 (Andreassen et al., 2012). Glaciological and geodetic mass balance for the period 1994-2008 was compared in Andreassen et al. (2016). The discrepancy found between glaciological and geodetic balance was not significant and did not call for a calibration.

This report gives a summary of the mass balance series including the homogenization process. The geodetic mass balance was calculated from LIDAR in 2008 and 2018. Thus the glaciological and geodetic mass balances were compared for the 10-year period 2008-2018.

Annual glacier front measurements showed that the glacier retreated 600 m from the start in 1998 to 2018. The recession was persistent for the entire period.

1.4 Outlook

The mass balance measurements at Langfjordjøkelen is reanalysed following the reanalyses scheme proposed by Zemp et al. (2013). The major steps were:

1. Analysis and scrutiny of glaciological and geodetic measurements (ch. 2)
2. Homogenization of glaciological and geodetic measurements (ch. 3)
3. Uncertainty assessment (ch. 4)
4. Validation of glaciological measurements against geodetic measurements (ch. 4)

The output of the reanalysis is a *homogenized glaciological mass balance time series* with an uncertainty assessment, and if calibration is required, a *calibrated glaciological mass balance time series*.

2 Observations

2.1 Geodetic mass balance

Geodetic mass balance for the periods 1966-1994 and 1994-2008 was reported in Andreassen et al. (2012).

LIDAR from September 2008 and September 2018 were used to produce detailed DTMs of the glacier surface of Langfjordjøkelen.

The GIS-data processing of maps and DTMs by NVE was done using ArcGIS 9.3/10.2 software (©ESRI) and Surfer software version 15.

2.1.1 Mapping 2008

LIDAR data were recorded on 9th September 2008 by Blom Geomatics AS (Blom Geomatics AS, 2008). Vertical aerial photographs were not taken. The LIDAR data was acquired using an Optech lidar instrument. The mean flying height was 2500 m above ground level. The scan rate was 20 Hz, the laser pulse rate 50 kHz and the scan angle 25 degrees, resulting in a mean point density of 0.6 points per m^2. The flight positioning was post-processed based on GNSS data from one reference station (Satref Skjervøy). Horizontal and vertical flight accuracy was not estimated, but the RMS value for the entire data set was estimated as 0.35 m and as <0.10 m for the glacier covered areas.

The data delivery from Blom Geomatics AS was point clouds (las and ascii) and glacier outlines based on the intensity values from the LIDAR data set. Due to some fresh snow (Fig. 2) the glacier outline was not complete.

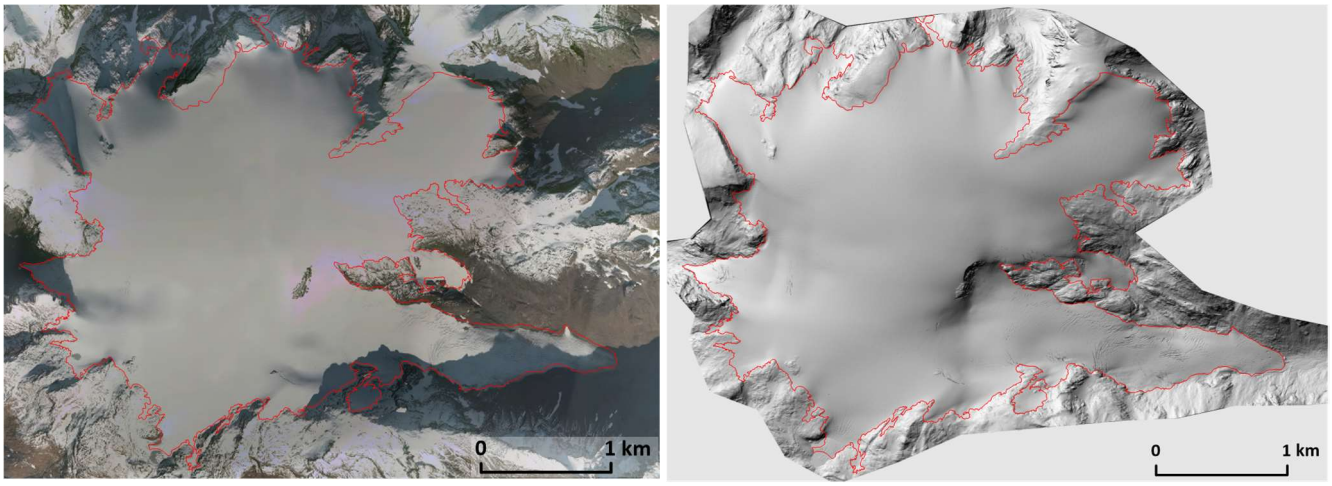

Figure 2
Orthophoto produced of aerial images from the period 9th-11th September 2008 to the left (source: norgeibilder.no) and shaded relief based on the DTM 2008 to the right. The glacier outline for 2008 in red.

The gridding method used for converting point cloud to regular grid data set was "Kriging". The regular grid data set (10x10 m) was used in the following calculations.

The glacier outlines delivered by Blom Geomatics were slightly revised and completed by NVE by using orthophoto from 9th-11th September 2008 (norgeibilder.no), a shaded relief of the DTM_{2008} (Fig. 2), and by using originally Landsat image from 2006. The ice

divide was determined from the DTM_{2008} using ArcGIS flow direction and flow accumulation tools.

All data was referred to the UTM co-ordinate system zone 34, Euref 89 datum and the Norwegian height system NN1954.

2.1.2 Mapping 2018

LIDAR data were recorded on 1st September 2018 by Terratec AS (Terratec AS, 2018). Due to technical problems vertical aerial photographs were not taken. The LIDAR data was acquired using a Riegl lidar instrument. The mean flying height was 2200 m above ground level. The scan rate was 175 Hz, the laser pulse rate 350 kHz and the scan angle 59 degrees, resulting in a mean point density of 2.0 points per m^2. The LIDAR data set from 2018 was compared with the data set from 2008 in stable areas. The control revealed a systematic vertical bias of 0.04 m. Thus the 2018 LIDAR data set was elevated 0.04 m. This control and calibration were done by Terratec. The homogeneity was described as good and the vertical accuracy was estimated as <0.10 m.

The data delivery from Terratec AS was point clouds (las and laz) and glacier outlines based on the intensity values from the LIDAR data set.

The gridding method used for converting point cloud to regular grid data set was "Kriging". The regular grid data set (10x10m) was used in the following calculations.

Optical satellite imagery from the Pleiades satellites on 1st September covering Langfjordjøkelen was available. Based on 0.5 m (black and white) and 2 m (colour) orthophotos produced from this imagery the glacier outlines were digitised. The outlines from the LIDAR data set (intensity values) and from the satellite imagery (orthophoto) were compared and evaluated (Fig. 3). The outlines assessed from the satellite imagery were considered as most reliable and thus, was preferred in the following calculations. However, the satellite imagery outlines were slightly revised by using a shaded relief of the DTM_{2018}. At the eastern outlet an area of debris covered ice is located at the southern side of the glacier snout (Fig. 4). The debris covered ice, which covers an area of 0.048 km^2, is not included in the glacier area.

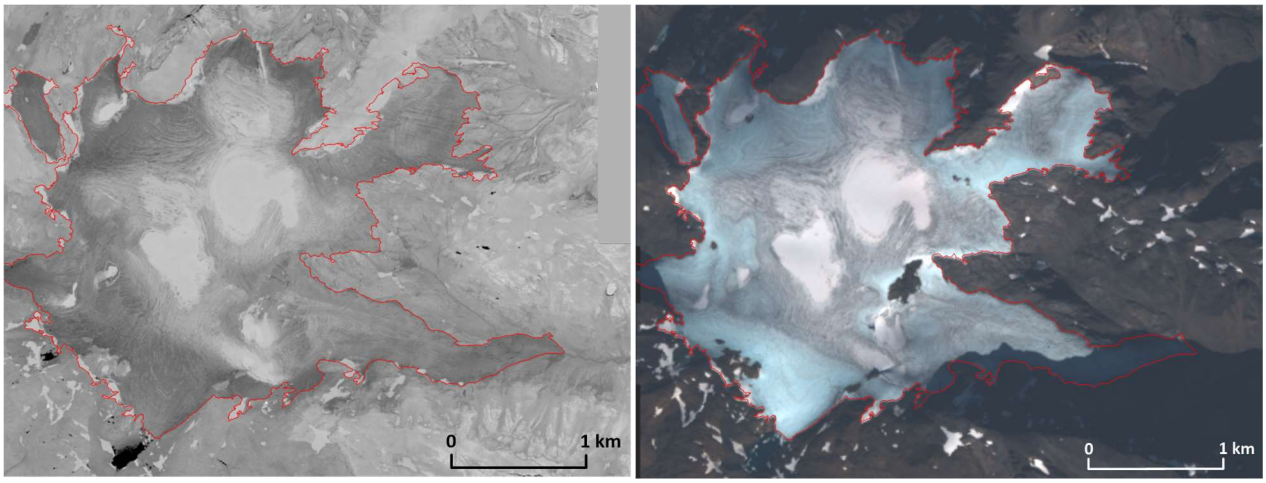

Figure 3
Raster image derived from the intensity values of the LIDAR data set to the left and orthophoto from the Pleiades satellite imagery (© CNES 2018, Distribution Airbus DS) to the right. The glacier outline for 2018 in red. Note the separated glacier area in northeast.

The ice divide was derived from the DTM_{2018} and compared with the current ice divide from DTM_{2008}. The differences between the two ice divides were negligible and thus, the 2008 ice divide was used in the following calculations.

Figure 4
The area of debris covered ice is located at the left side of the glacier snout (see the arrow). Photo: Miriam Jackson.

All data was referred to the UTM co-ordinate system zone 34, Euref 89 datum and the Norwegian height system NN1954.

2.1.3 Density

Determination of a density conversion factor was required in order to convert the volume change of snow, firn and ice to mass change. It is common to assume a constant density profile in the accumulation area, following Sorge's law (Bader, 1954). Hence, density of glacier ice, 900-917 kg m^{-3} (Cuffey and Paterson, 2010), is often used for the conversion (e.g. Haug et al., 2009 and Andreassen, 1999). This assumption however, is valid only under steady-state conditions and was considered to be a maximum estimate in this study. Assuming a value of 850 ±60 kg m^{-3} to convert volume change to mass change is found to be appropriate for a wide range of conditions (Huss, 2013). Hence, this value was used for the conversion of the volumetric changes into water equivalent.

2.1.4 Adjustment for different dates

Comparison of glaciological and geodetic mass balance required an adjustment because the field measurements and aerial surveys were acquired at different dates. The related difference depends on the changes in surface elevation between the field and aerial surveys. Accordingly, increasing time span will result in increasing difference. The season (summer/ autumn) and the general mass turn over will also influence the difference. Dates for field measurements and aerial surveys and corresponding adjustments are shown in table 1.

Table 1
Survey dates and adjustments for 2008 and 2018.

year	date			correction	
	LIDAR	field survey$_{summer}$	field survey$_{autumn}$	category	ΔB_s (m w.e.)
2008	9th September	5th August	16th October	melting	−0.19
2018	1st September	15th August	12th October	melting	−0.53

In 2008 the lidar data was acquired 9th September. The stakes were measured 5th August and the final ablation was measured on 16th October. The melting for the period from 5th August to 16th October was measured on five stakes. Based on these stake measurements and temperature measurements from the meteorological station Langfjordjøkelen (915 m a.s.l.) the melting for the period from 9th September to 16th October was estimated. Fresh snow at the time of ablation measurement on 16th October was not included in the 2008 annual mass balance and was, hence not taken into account in this adjustment.

In 2018, the lidar survey date was 1st September. The stakes were measured 15th August and the final ablation was measured on 12th October. The melting for the period from 15th August to 12th October was measured on six stakes. Based on these stake measurements and temperature measurements from the station Langfjordjøkelen the melting for the period from 1st September to 12th October was estimated. Fresh snow at the time of ablation measurement on 12th October was not included in the 2018 annual mass balance and was, hence not taken into account in this adjustment.

According to the estimated melting from the lidar survey dates to the field survey dates, the geodetic mass balances were adjusted as:

– date adj.$_{2008}$ + date adj.$_{2018}$

2.1.5 Glacier boundaries

The hydrological basin was used for the glaciological mass balance calculations. This means that the entire glacier area within the hydrological catchment of the lake Andrevatnet (Fig. 1) was included. The hydrological drainage basins for the two years 2008 and 2018 are quite different in area extent. The ice divides from 2008 and 2018 are quite similar and thus the ice divide from 2008 was used for both DTMs. The hydrological basin area is 3.2 km^2 (2008) and 2.6 km^2 (2018), respectively. For the geodetic volume change calculations a combination of the glacier boundaries was used so that the analyses mask will surround both glacier areas. Areas within the glacier basin defined as rock in both years were not included.

2.2 Glaciological mass balance

Glacier surface mass balance at Langfjordjøkelen has been monitored annually since 1989 with exception of the two years 1994 and 1995. The extent of measurements has varied over time, but the method of calculation has been the same for the whole period. The measurements and calculations are in principle based on methods from Østrem and Brugman (1991) and as described in Andreassen et al. (2005) and Kjøllmoen et al. (2018).

The measurements are reported in “Glaciological investigations in Norway”, which are annual reports published by NVE. A homogenized mass balance series for Langfjordjøkelen 1989-2009 was reported in Kjøllmoen et al. (2016).

2.2.1 Monitoring program and field measurements

The annual mass balance measurements started in May 1989 (Østrem et al., 1991).

Normally, winter balance measurements were carried out from late April to late May, while the annual balance measurements were carried out from late September to late October. Winter balance was measured using a number of stakes, as well as doing a number of snow depth soundings to the late-summer surface from previous year. In addition to snow depth, snow density was measured in one vertical profile (Fig. 5). The snow density measurements were done at the same time as the snow depth measurements. Annual balance was measured by stake readings.

Figure 5
Snow density measurements in May 2011. Photo: Ragnar Ekker.

The number of stakes and snow depth measurements has varied some over the years from the beginning in 1989 to present (Fig. 6 and Tab. 2).

In the first five years (1989-93) a network of 2-4 stakes was maintained and the snow depth was measured in 16-53 points along one profile from the glacier terminus to the glacier summit.

From 1996, the number of stakes was extended to 4-6, and the number of snow depth measurements was between 46 and 118 points along two parallel profiles from the glacier terminus to the glacier summit. The snow density was determined in one location for the whole period.

Up to 2013, the snow depths were measured in random points along two profiles. From 2014, the random points were replaced by fixed points along the two profiles giving about 60 points.

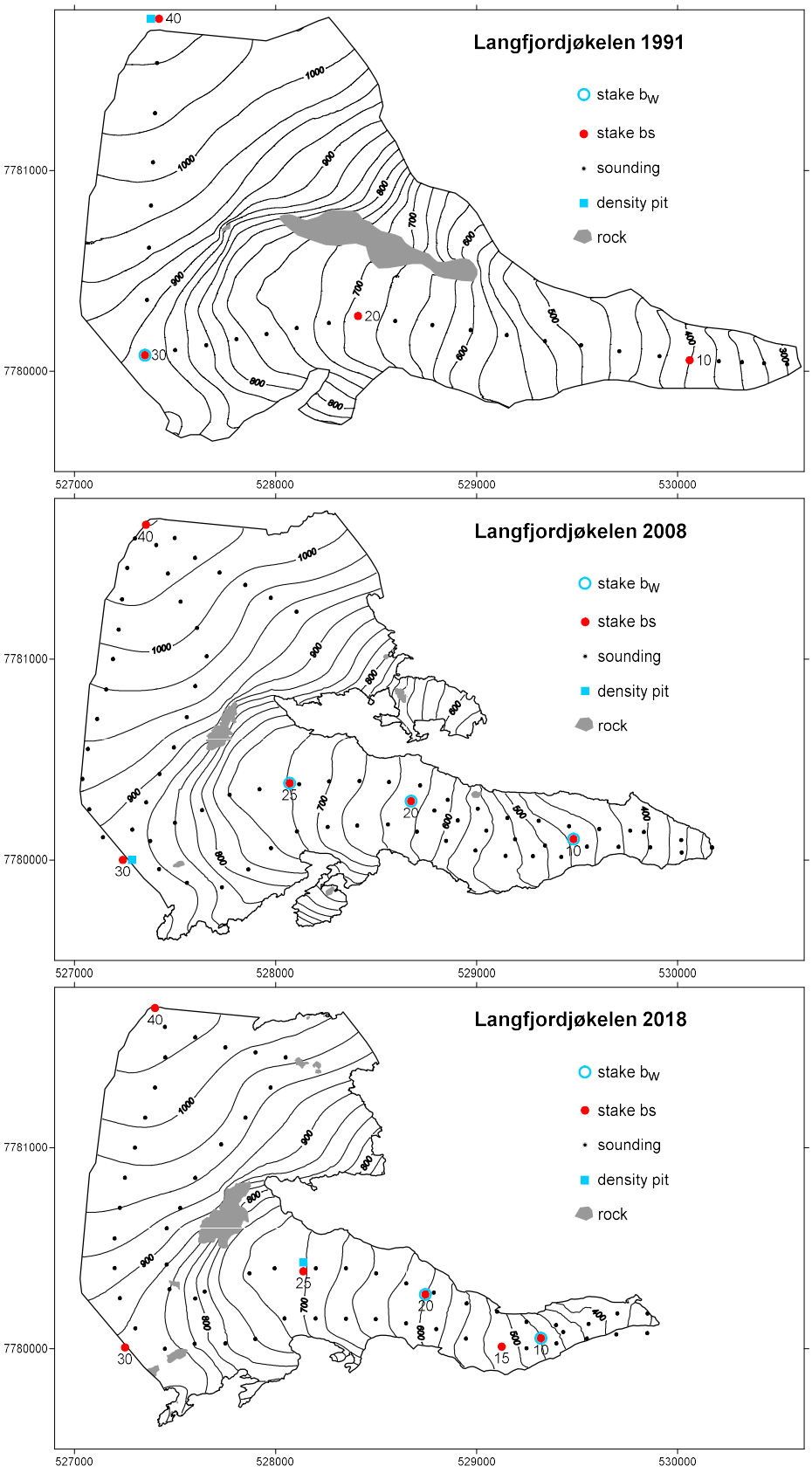

Figure 6
Typical stake network and snow depth soundings representing three different periods. Upper: 1991 (1989-93), middle: 2008 (1996-2013) and lower: 2018 (2014-18). Non-glaciated areas within the basin are shaded in grey.

Table 2
A summary of the annual mass balance measurements at Langfjordjøkelen during the period 1989-2018.

Year	Date		Stakes (number)			Density pit			Snow depth measurements				Data
	spring	autumn	b_w	b_s	b_a	position	depth (m)	ρ (kg m^{-3})	number	$\bar{x}$ (m)	min. (m)	max. (m)	quality
1989	24th May	19th Oct.	0	2	2	40	5.71	509	41	4.5	1.6	8.5	Medium
1990	24th May	5th Sep.	0	4	4	40	5.78	435	49	5.7	2.7	7.2	Good
1991	14th May	4th Oct.	1	4	4	40	4.77	455	29	4.6	2.6	6.2	Medium
1992	3rd June	22nd Sep.	2	4	4	40	5.01	594	16	4.2	1.6	7.7	Medium
1993	15th May	24th Sep.	0	2	4	40	5.49	453	53	5.3	3.4	7.0	Medium
1996	24th May	16th Oct.	0	4	4	30	4.58	485	112	4.4	2.5	7.0	Good
1997	10th June	2nd Oct.	2	4	4	30	4.10	534	118	4.5	2.7	6.4	Medium
1998	3rd June	30th Sep.	1	4	4	30	4.42	455	77	3.8	0.9	5.6	Good
1999	25th May	25th Sep.	3	5	5	30	3.09	471	82	2.6	0.7	4.2	Good
2000	23rd May	11th Oct.	5	5	5	30	4.63	501	94	4.8	2.4	7.2	Good
2001	6th June	7th Oct.	4	5	5	30	2.49	488	78	2.8	1.0	4.3	Good
2002	24th May	12th Oct.	3	5	5	30	3.87	510	88	4.2	1.5	6.3	Good
2003	24th May	2nd Oct.	4	4	5	30	4.23	526	73	4.5	2.1	6.5	Good
2004	29th Apr.	4th Oct.	5	5	5	30	2.60	450	74	3.5	1.5	5.7	Medium
2005	26th May	26th Oct.	5	5	5	30	3.84	478	83	4.0	1.8	6.3	Medium
2006	25th Apr.	6th Oct.	4	5	5	30	3.07	405	73	3.3	1.7	4.6	Medium
2007	22nd May	3rd Nov.	4	5	5	25	4.15	504	85	4.2	1.8	6.1	Good
2008	22nd May	16th Oct.	3	5	5	30	3.48	466	81	3.2	1.7	4.8	Good
2009	7th May	7th Oct.	4	5	5	25	3.03	460	70	3.9	1.9	5.9	Good
2010	19th May	23rd Sep.	4	5	5	30	2.00	515	75	3.4	1.7	5.0	Good
2011	11th May	20th Sep.	1	6	6	30	3.15	460	65	4.6	3.0	6.1	Medium
2012	19th Apr.	25th Sep.	6	6	6	25	2.50	348	81	3.3	1.8	6.2	Good
2013	14th May	7th Nov.	1	5	6	25	4.15	448	46	4.4	2.9	6.3	Good
2014	9th May	24th Sep.	2	6	6	25	4.47	463	60	4.9	3.4	7.0	Good
2015	8th May	23rd Sep.	5	6	6	25	3.30	485	60	3.8	1.6	6.4	Medium
2016	23rd May	22nd Sep.	2	6	6	25	3.27	521	60	2.9	0.8	4.9	Good
2017	25th Apr.	29th Sep.	0	6	6	25	4.23	418	62	4.6	2.1	7.1	Good
2018	10th May	12th Oct.	2	6	6	25	3.24	489	61	3.0	1.0	3.9	Good

2.2.2 Mass balance calculation

The mass balance was in principal calculated using a stratigraphic system, i.e. between two successive summer surfaces, as described in Cogley et al. (2011). The spatial interpolation of point measurements was done by estimating accumulation and ablation in elevation intervals of 50 m vertical resolution. The altitudinal mass balance curves were made by plotting point measurements of winter, summer and annual balance versus altitude. Representative values for each 50-m elevation interval were then extracted from these scatter plots (Fig. 7). The method is called the profile method.

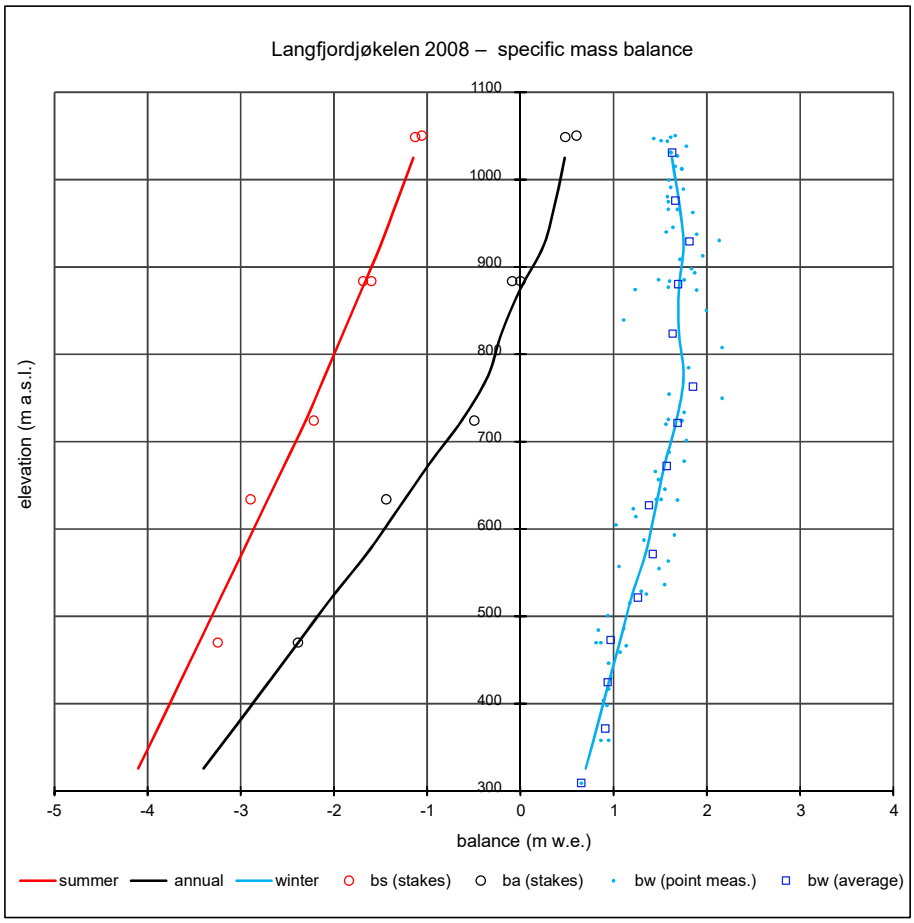

Figure 7
The altitudinal winter, summer and annual balance curves are plotted versus altitude. Point values for b_w (•), b_s (○) and b_a (○), together with average b_w (□) for each 50 m height interval are also plotted. This calculation method has been used for the whole period. The example diagram above is from 2008.

2.2.3 Glacier boundaries

The boundaries used for glaciological mass balance measurements and calculations can be defined by the hydrological basin or the glaciological basin. While the hydrological basin includes the entire glacier area within a certain hydrological catchment, the glaciological basin is limited to the glacier area providing ice to a defined glacier tongue. Independent of whether a hydrological or glaciological basin is used, the drainage boundary is defined by the ice margin and the drainage divide. The drainage divide can be defined in two different ways; either calculated from the glacier surface topography (ice drainage divide) or from a combination of subglacial topography and ice thickness (water drainage divide).

For Langfjordjøkelen the mass balance was measured and calculated using the hydrological basin draining to the lake Andrevatnet (Fig. 1). The drainage divide was solely calculated from the glacier surface topography.

In the reported original datasets as published up to and including 2017 (Kjøllmoen, 2018), the mass balance calculations are based on the height-area distribution from 1966, 1994 and 2008 maps (Fig. 8). As shown in the figure, there are some time lags between the mass balance data and the reference area used for calculating mass balances. When a new

map was available, it was used for the calculations from then and onwards. The mass balance series for the period 1989-2009 was homogenised in 2016 (Kjøllmoen, 2016).

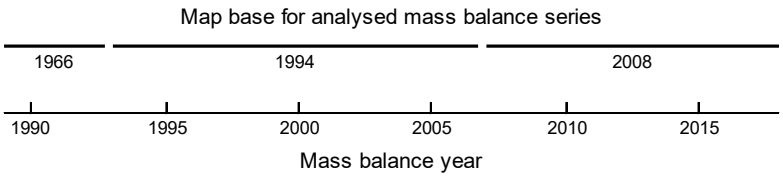

Figure 8
Upper line indicates map base used in the reported original mass balance series. Years denote year of validity period for each map.

2.2.4 Glaciological mass balance series

The reported original glaciological mass balance series (included estimated values for 1994 and 1995) gives a deficit of −27.2 m w.e. for the period 1989-2017. The results show a considerable mass loss from 1997 to 2017 (−26.2 m w.e.). The years 1989-1996 were nearly in balance (−1.0 m w.e.).

The mean winter, summer and annual mass balances for 1989-2017 were 2.05, −3.04 and −0.99 m w.e., respectively. The original annual winter, summer and annual mass balance results from 1989 to 2017 are shown in figure 9.

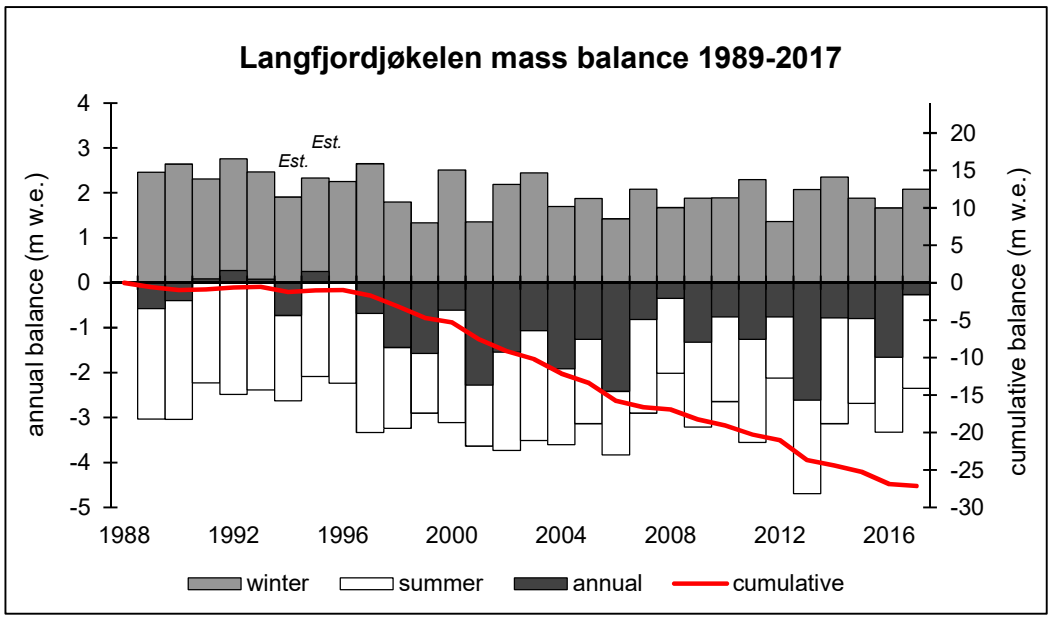

Figure 9
Original winter, summer and annual mass balance for Langfjordjøkelen over the period 1989-2017.

3 Homogenization

3.1 Geodetic mass balance

The accuracy of the final DTMs is principally influenced by the quality of the raw data and by the process from raw data to DTM. The raw data acquisition and the DTM processing were quite similar for 2008 and 2018.

3.1.1 Mapping 2018

The 2018 DTM was based on data acquired by LIDAR (see chap. 2.1.2). Generally, the accuracy of data sets acquired by LIDAR is of high quality. The accuracy of the LIDAR data was investigated by comparing the original LIDAR data set with five control points measured by static GNSS and more than 8000 profile points measured by kinematic GNSS on the glacier surface. As the x and y co-ordinates of the original LIDAR point values versus GNSS points are not exactly identical, interpolated values were extracted from the LIDAR data set. The interpolation was done using the "Kriging" interpolation method and a grid size of 2x2 m.

The profile points and three control points were measured on 15th August, while the LIDAR data was acquired on 1st September. Four control points were also measured on 12th October. Based on stake readings on 15th August and 12th October, and air temperature from the climate station Langfjordjøkelen (915 m a.s.l.), the elevation changes for the profile points and control points were estimated for the period from 15th August to 1st September. The accuracy of the estimated elevation changes was assumed as ±0.10 m. The elevation changes from 15th August to 1st September are calculated irrespective of the ice dynamics. The results from the comparison are shown in table 3 and figure 10. Five control points and 8288 profile points on the glacier surface were compared. The accuracy of the static control points was assumed as ±0.10 m, while the accuracy of the kinematic profile points was assumed as ±0.25 m. Unreliable profile points with solution type "Code Diff" and "Float", and with Standard Deviation greater than 0.25 m were omitted. The differences (Diff. = $Height_{adj.}$ – $Height_{LIDAR}$) for the five control points were between +0.12 and −0.27 m with an average of −0.10 m. The differences for the profile points were between +0.67 and −0.87 m with an average of −0.05 m.

Table 3
Comparison of glacier surface elevation between control points measured with static GNSS and the original LIDAR data set. The surface elevations measured on 15th August and 12th October ($Height_{GNSS}$) were adjusted to elevations related to 1st September ($Height_{adj.}$).

Point No.	North	East	$Height_{GNSS}$	$Height_{adj.}$	$Height_{LIDAR}$	Diff. (m)
Measured 15th August						
15-13	7 780 011.48	529 129.24	513.75	513.11	512.99	0.12
25-13	7 780 386.15	528 139.15	702.57	702.10	701.98	0.12
30-13	7 780 005.79	527 251.25	871.14	870.61	870.80	-0.19
Measured 12th October						
15-13	7 780 012.59	529 130.17	511.87	512.67	512.76	-0.09
20-18	7 780 275.56	528 746.59	599.75	600.58	600.65	-0.07
30-13	7 780 005.60	527 251.28	870.13	870.75	870.78	-0.03
40-05	7 781 696.23	527 399.60	1 041.36	1 041.77	1 042.04	-0.27

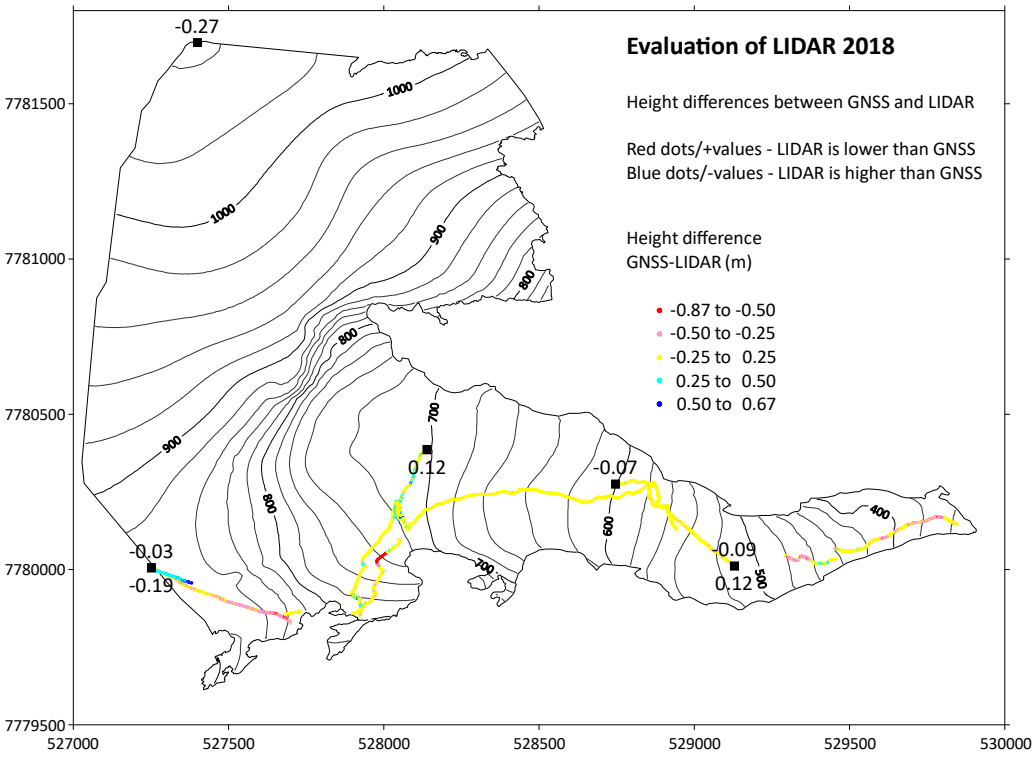

Figure 10
Spatial distribution of 8288 profile points and five control points measured on the glacier surface of Langfjordjøkelen on 15th August and 12th October. Control point values below the point symbol is measured 15th August and above is measured 12th October.

The evaluation based on the kinematic profile GNSS measurements on the glacier surface revealed differences up to 0.87 m. Due to the time lag between the GNSS measurements and the LIDAR acquisition, the estimated surface elevation change from 15th August to 1st September is an uncertain factor and can possibly explain some of the differences. Another source of error is that the GNSS receiver/antenna was carried on top of a rucksack (Fig. 11). when walking on the ice surface. Thus the antenna height could vary some decimetre when walking on the rough ice surface, e.g when passing small crevasses. The comparison based on the static control points however, gave differences less than 0.3 m.

Figure 11
Kinematic GNSS profile measurements on 15th August. The receiver/antenna (see the circle) was carried in a rucksack.
Photo: Miriam Jackson.

Generally, the two evaluations showed good accordance between the control and profile points, and the LIDAR data. Accordingly, the quality of the LIDAR data was considered as good.

3.1.2 Mapping 2008

As the 2018 DTM, the 2008 DTM was also based on data acquired by LIDAR. At the time of aerial surveying (9th September 2008) no independent GNSS measurements were done.

The 2008 LIDAR data however, was compared with the 2018 DTM in stable non-glacierized areas. The 2018 DTM was then considered as the reference DTM. Ideally the non-glacierized terrain from two DTMs should correspond exactly. Due to all the inaccuracies, however, elevation differences will always occur when comparing two DTMs.

At the time of aerial survey in September 2008, there was some fresh snow above 700 m altitude. Thus the comparison of the 2008 LIDAR data with the 2018 DTM was solely located to the lower areas in east (Fig. 12). The results from 641552 grid points (1x1 m) were first compared. The grid cell differences (Diff. = $Z_{DTM2008} - Z_{DTM2018}$) were between +12.1 and −12.8 m with an average of −0.04 m. The standard deviation was 0.49 m.

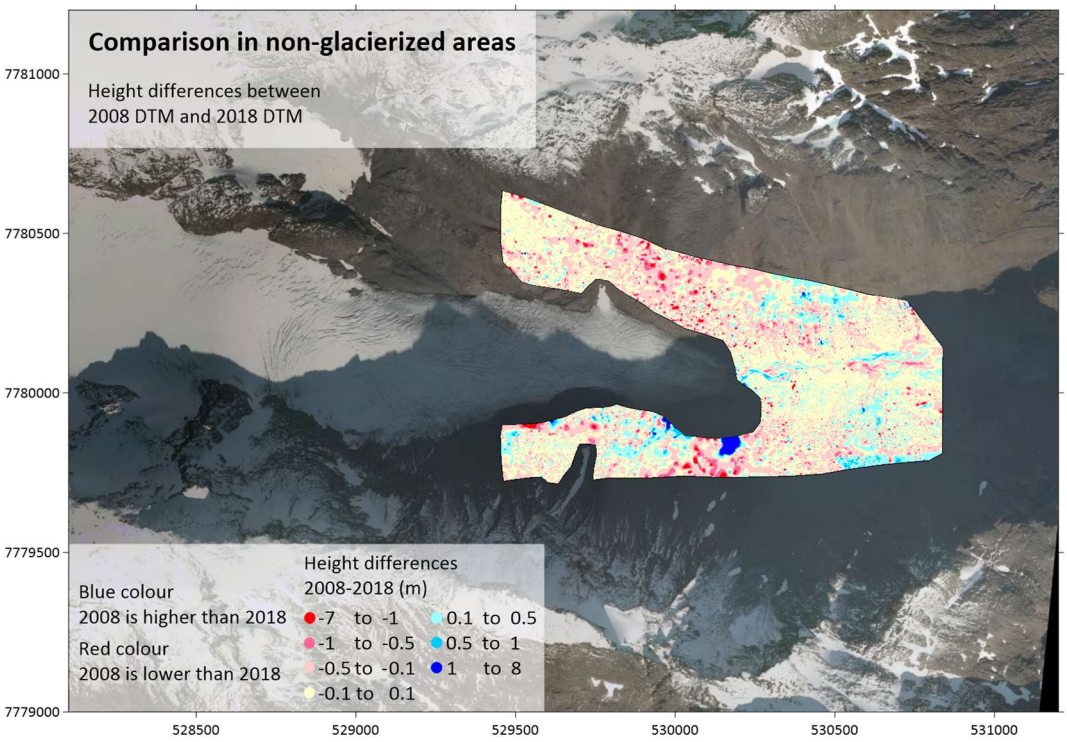

Figure 12
Aerial distribution of elevation differences in non-glacierized areas by comparing the 2008 DTM with the 2018 DTM. Thus, blue colour indicate that the 2008 DTM is higher than the 2018 DTM and vice versa. Values in areas steeper than 30° were removed.

Comparing elevation values in steep areas is considered to be very uncertain and should preferably be avoided. Thus, all difference values located in areas steeper than 30° were removed. Accordingly, the results from the 244558 remaining points showed differences from +8.0 to −7.0 m with an average of −0.04 m. The standard deviation was 0.27 m. Generally, the results indicated that the 2008 DTM and the 2018 DTM (Fig. 12) are quite

similar in non-glacierized areas. The maximum (+8.0 m) and minimum (−7.0 m) differences are rather great, but the average difference (−0.04 m) is very low and better than the given accuracy for the laser points (0.10 m). The reasons for the highest differences can be that the terrain is not stable, and reflection errors from sloping areas. Factors like material (gravel) from landslides, erosion in the glacial river and ice-cored moraines will influence the surface elevation. However, in accordance with the evaluation of the 2018 DTM, both DTMs are proved to be of high quality.

3.1.3 Mass change 2008-2018

The spatial distribution of thickness changes at Langfjordjøkelen from 9th September 2008 to 1st September 2018 is shown in figure 13. The geodetic mass balance over the period 2009(08)-2018 was calculated within the hydrological basin using grid size of 10 x 10 m. Average volume change is multiplied with the density conversion factor (850 kg m^{-3}), divided with the mean area for 2008 and 2018, and adjusted for additional melting in 2008 and 2018. The results are given in table 4.

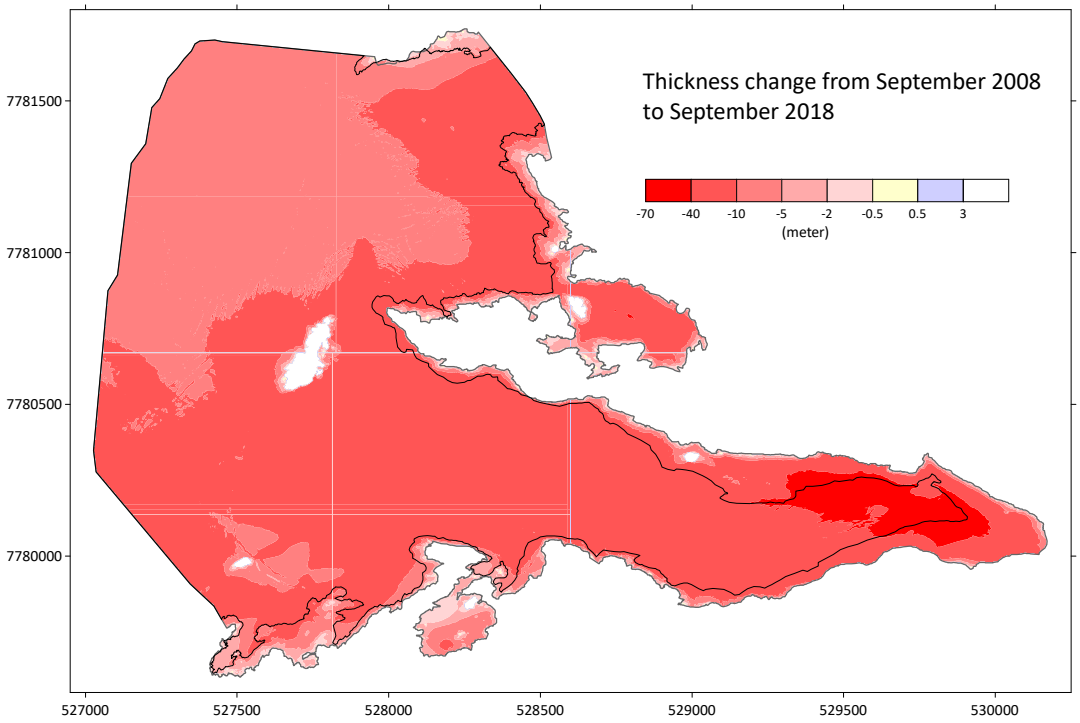

Figure 13
DTM differences within the hydrological basin of Langfjordjøkelen from 9th September 2008 to 1st September 2018. The glacier extents from 2008 (grey line) and 2018 (black line) are also shown.

Geodetic mass balance over 2008-2018 was −13.85 ±1.52 m w.e. In accordance with the geodetic mass balance deficit, the ice thickness change was significant negative (>−0.5 m) for 99.7 % of the surveyed glacier area (Fig. 13). Hence a decrease of ice thickness appeared all over the glacier surface. Mean thickness change was −14.4 meters.

Table 4
Volume change and geodetic mass balance for the east-facing part of Langfjordjøkelen from 2008 to 2018.

period	$area_{2008}$	$area_{2018}$	vol. ch.	dens. fac.	date adj. (m w.e.)		geod. mb. (m w.e.)	
glacier	(km^2)	(km^2)	(mill. m^3)	(kg m^{-3})	2008	2018	acc.	ann.
2008-2018								
Langfjordjøkelen	3.19	2.61	-46	850	-0.19	-0.53	-13.85	-1.39

$area_{2008}$ is the area of the east-facing part of Langfjordjøkelen in September 2008.
$area_{2018}$ is the area of the east-facing part of Langfjordjøkelen in September 2018.
vol. ch. is the volume change of ice, firn and snow over the given period.
dens. fac. is the density used for converting from ice, firn and snow to water equivalent.
date adj. is a correction for different dates for mapping and field survey for each year in the period.
geod. mb. is accumulated (acc.) and annual (ann.) balance for the period.

3.2 Glaciological mass balance

As new DTMs from 2018 and 2008 were available, the mapping from 1994 was improved, and some minor changes of the methodology of the surface mass balance calculations has been implemented through the years since the beginning in 1989, a homogenization of the series of Langfjordjøkelen was necessary. Three major factors were considered and are described in the following.

3.2.1 Height-area distribution

The original mass balance calculations were based on height-area distribution from three maps (1966, 1994 and 2008). There were some time lags between the mass balance data and the map used for the calculations (Fig. 8). The period between two mappings was divided in two, and each map was applied to half of the period before the mapping year and half of the period after the mapping year (Fig. 14). Another method for assessing the height-area distribution is an annual linear change-over from DEM_I to DEM_{II}. This method was tested and gave nearly the same result as the chosen method (Andreassen et al., 2012). Accordingly, the homogenization involved re-calculation of the periods 1989-93, 2002-07 and 2014-17.

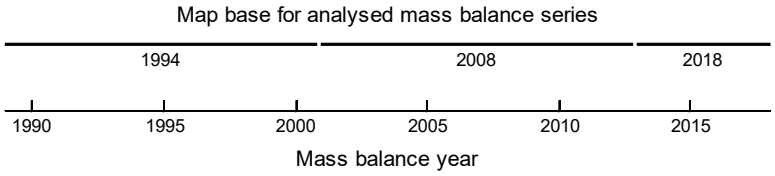

Figure 14
Upper line indicates map base for the re-analysed mass balance series. Years denote year of validity period for each map.

3.2.2 Converting from snow depth to water equivalent

Winter balance calculations are based on measurements of snow depths and snow density (described in chapter 2.2.1). The converting procedure from snow depth to water equivalent has varied through the ages. For the first seven years (1989-93 and 1996-97) a Unix (computer operating system) based model was used in the converting process. For the next three years (1998-2000) a precise documentation of the converting procedure is lacking. From 2001 different variants of the current converting method was adopted. The snow density and, hence, the water equivalent, was calculated for each snow sample part. The accumulated water equivalent was plotted with increasing snow depth and a

mathematical trend line and function was formatted. Usually a polynomial of degree three, two or one was used, e.g expressed as: $b_w = a*c_a^3 + b*c_a^2 + c*c_a + d$ (a, b, c and d are coefficients). An example from 2014 is given in figure 15. In the homogenization the converting method using a polynomial of degree three or two was implemented for the years 1989-93, 1996-2009 and 2014. For 2005 a polynomial function was illogical, and hence, a linear function was used.

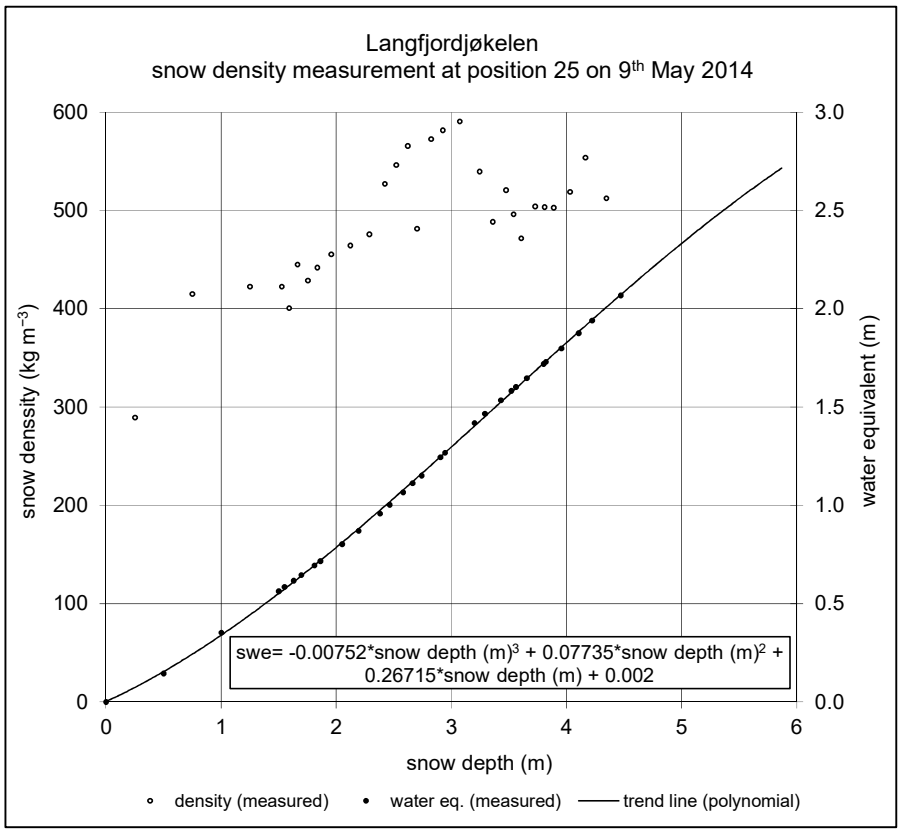

Figure 15
Snow density measurements from 2014. The snow density for each sample part is shown on the left axis and the accumulated water equivalent is shown on the right axis. The converting function is shown in the frame.

3.2.3 Ice divide

The ice divide was originally constructed for each map, including the 1966 and 1994 maps. It was, however, assumed that the ice divide constructed from the 2008 DTM, and later confirmed with the 2018 DTM, was the most accurate and approximately unchanged in the entire period. Accordingly, the homogenization involved re-calculation of the periods 1989-93 and 1996-2007 using the ice divide from 2008.

3.2.4 Results

Homogenizing by re-calculation of the mass balance series from 1989 to 93, 1996 to 2009 and 2014 to 2017 (the years 2010-2013 and 2018 were not necessary to re-calculate) ensure a uniform methodology, data processing and interpretation of the calculation process from field data to the final balance values. The re-calculation was based on the profile method within the hydrological basin and with the current DTM and ice divide from 2008.

The original and homogenized mass balance series over the period 1989-2018 are shown in table 5 and figure 16.

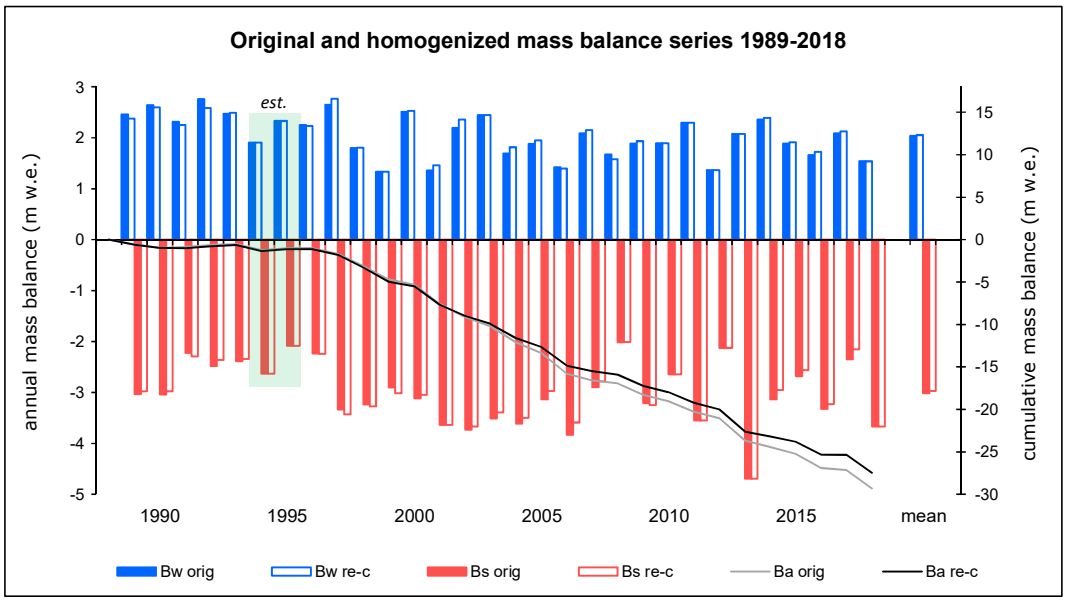

Figure 16
Original and homogenized mass balance series for the period 1989-2018.

The original and homogenized mass balance series over the period 1989-2018 shows a deficit of −29.3 m w.e. and −27.5 m w.e., respectively. The cumulative winter balance increased by 0.4 m w.e., while the change in cumulative summer balance was 1.4 m w.e.

Generally, the homogenized mass balance series over 1989-2018 gave slightly greater annual winter balances and slightly lower summer balances than the original series. The mean winter balance increase was 0.017 m w.e. per year, and the mean summer balance decrease (absolute value) was 0.062 m w.e. per year. The impact of the three major changes in methodology was not tested thoroughly, but some few spot checks indicated rather small changes in annual balances, typical within ±0.1 m w.e.

Table 5
Original and homogenized mass balance series over the period 1989-2018.

	Original mass balance series								Homogenised mass balance series								Homogenised in relation to		
Year	B_w	B_s	B_a	ΣB_a	ELA	AAR	DTM	Area	B_w	B_s	B_a	ΣB_a	ELA	AAR	*DTM	Area	[1)]DTM	[2)]Dvd	[3)]Dens
1989	2.46	-3.03	-0.57	-0.57	865	47	1966	4.80	2.38	-2.98	-0.60	-0.60	890	39	1994	3.62	x	x	x
1990	2.64	-3.04	-0.40	-0.97	780	53	1966	4.80	2.60	-2.98	-0.38	-0.98	835	49	1994	3.62	x	x	x
1991	2.31	-2.23	0.09	-0.89	680	67	1966	4.80	2.25	-2.29	-0.04	-1.02	730	64	1994	3.62	x	x	x
1992	2.76	-2.49	0.27	-0.61	690	64	1966	4.80	2.58	-2.37	0.22	-0.80	705	68	1994	3.62	x	x	x
1993	2.47	-2.39	0.08	-0.54	700	64	1966	4.80	2.49	-2.34	0.15	-0.65	745	62	1994	3.62	x	x	x
1994	*1.91*	*-2.63*	*-0.73*	*-1.26*	*849*	*46*	*1994*	*3.65*	*1.91*	*-2.63*	*-0.73*	*-1.38*	*849*	*47*	*1994*	*3.62*			
1995	*2.33*	*-2.09*	*0.25*	*-1.02*	*698*	*69*	*1994*	*3.65*	*2.33*	*-2.09*	*0.25*	*-1.13*	*698*	*69*	*1994*	*3.62*			
1996	2.25	-2.23	0.02	-1.00	700	69	1994	3.65	2.23	-2.24	-0.01	-1.15	735	64	1994	3.62		x	x
1997	2.65	-3.34	-0.69	-1.69	820	50	1994	3.65	2.77	-3.43	-0.66	-1.81	805	53	1994	3.62		x	x
1998	1.80	-3.24	-1.44	-3.13	>1050	0	1994	3.65	1.81	-3.27	-1.47	-3.28	>1053	0	1994	3.62		x	x
1999	1.33	-2.91	-1.57	-4.70	970	22	1994	3.65	1.33	-3.02	-1.68	-4.96	1025	8	1994	3.62		x	x
2000	2.51	-3.12	-0.61	-5.31	860	44	1994	3.65	2.53	-3.05	-0.52	-5.48	850	47	1994	3.62		x	x
2001	1.36	-3.64	-2.28	-7.59	>1050	0	1994	3.65	1.46	-3.64	-2.18	-7.67	>1053	0	1994	3.62		x	x
2002	2.19	-3.73	-1.54	-9.13	>1050	0	1994	3.65	2.36	-3.67	-1.31	-8.98	>1050	0	2008	3.22	x	x	x
2003	2.44	-3.51	-1.07	-10.20	>1050	0	1994	3.65	2.45	-3.39	-0.95	-9.93	>1050	0	2008	3.22	x	x	x
2004	1.69	-3.61	-1.92	-12.11	>1050	0	1994	3.65	1.81	-3.50	-1.69	-11.62	>1050	0	2008	3.22	x	x	x
2005	1.88	-3.14	-1.26	-13.37	940	28	1994	3.65	1.95	-2.97	-1.02	-12.64	945	29	2008	3.22	x	x	x
2006	1.42	-3.83	-2.42	-15.78	>1050	0	1994	3.65	1.39	-3.59	-2.20	-14.84	>1050	0	2008	3.22	x	x	x
2007	2.09	-2.90	-0.81	-16.60	870	72	1994	3.65	2.15	-2.79	-0.64	-15.48	880	44	2008	3.22	x	x	x
2008	1.67	-2.02	-0.35	-16.95	835	53	2008	3.22	1.58	-2.01	-0.43	-15.91	875	45	2008	3.22			x
2009	1.89	-3.21	-1.32	-18.27	>1050	0	2008	3.22	1.93	-3.25	-1.31	-17.22	>1050	0	2008	3.22			x
2010	1.89	-2.65	-0.76	-19.03	1005	12	2008	3.22	1.89	-2.65	-0.76	-17.97	1005	12	2008	3.22			
2011	2.30	-3.55	-1.26	-20.28	>1050	0	2008	3.22	2.30	-3.55	-1.26	-19.23	>1050	0	2008	3.22			
2012	1.37	-2.13	-0.76	-21.04	950	27	2008	3.22	1.37	-2.13	-0.76	-19.99	950	27	2008	3.22			
2013	2.08	-4.69	-2.62	-23.66	>1050	0	2008	3.22	2.08	-4.69	-2.62	-22.61	>1050	0	2008	3.22			
2014	2.36	-3.14	-0.78	-24.44	>1050	0	2008	3.22	2.39	-2.95	-0.56	-23.17	940	33	2018	2.61	x		x
2015	1.88	-2.68	-0.80	-25.24	1025	6	2008	3.22	1.92	-2.57	-0.65	-23.82	1020	6	2018	2.61	x		
2016	1.66	-3.33	-1.66	-26.90	>1050	0	2008	3.22	1.72	-3.23	-1.51	-25.32	>1043	0	2018	2.61	x		
2017	2.08	-2.35	-0.27	-27.17	810	56	2008	3.22	2.12	-2.15	-0.03	-25.35	780	65	2018	2.61	x		
2018	1.54	-3.67	-2.13	-29.30	>1043	0	2018	2.61	1.54	-3.67	-2.13	-27.48	>1043	0	2018	2.61			

*The ice divide from 2008 was used for all DTMs.
[1)] **DTM** indicates whether the map base of the recalculated mass balance series is changed.
[2)] **Dvd** indicates whether the ice divide from 2008 is used for the recalculation.
[3)] **Dens** indicates whether the conversion from snow depth to water equivalent is based on a modified trend line model.

4 Comparison of glaciological and geodetic mass balance

Glaciological and geodetic mass balance for Langfjordjøkelen are compared for the period 2009-2018 (autumn 2008 to autumn 2018). Glaciological mass balance is based on annual measurements of snow depth and snow density at the end of the winter, and of ablation measurements at the end of the summer. Geodetic mass balance is based on changes in elevation and area between two mappings.

In order to compare glaciological and geodetic mass balance, the errors for the different methods and the internal melting were estimated. Internal melting was estimated using the methods described in Oerlemans (2013) and Alexander et al. (2011), and applied for ten glaciers in Norway in Andreassen et al. (2016). For this purpose internal melting is expressed as melting inside and underneath the glacier due to heat of dissipation. Melting due to rain was considered negligible, as most of this melting affects snow, firn and ice at the surface, rather than the subglacial system.

Internal melting (*B int*) was calculated for each elevation interval (50 meter) used in the surface mass balance by the formula

$$B\ int = \frac{\sum_h g * ph * ah * (h - bL)}{A * Lm}$$

where g is the acceleration of gravity, h is mean elevation of elevation interval used in surface mass balance calculations, ph is precipitation at h, ah is glacier area of elevation interval h, bL is bed elevation at glacier snout, A is total glacier area og Lm is latent heat of fusion.

Precipitation was defined as a linear function of elevation. Daily precipitation was extracted from www.senorge.no, and the gradient was selected to give an annual precipitation 1.5 times the measured winter balance.

The internal melting at Langfjordjøkelen was quantified as −0.04 m w.e. a^{-1} (Andreassen et al., 2016). The uncertainty, $\sigma.B.\ int$, was assumed to be one third of the estimated internal melting, which amounts to ±0.01 m w.e. a^{-1}.

In order to compare, the uncertainty of the measurements was estimated in accordance with Zemp et al. (2013) and Andreassen et al. (2016).

The results from glaciological and geodetic mass balance, together with internal melting, are shown in table 6.

The results show a difference between glaciological and geodetic mass balance (Δ) as 0.19 m w.e. a^{-1} for 2008-2018.

Table 6
Comparison of glaciological and geodetic mass balances and results of the uncertainty analysis for Langfjordjøkelen over the period 2008-2018. All mass balances and errors are in m w.e. a^{-1}.

glacier	years	B glac.	σ.glac. point	σ.glac. spatial	σ.glac. ref	B geod.	σ.geod. DTM	σ.dc	B int	σ.B. int	Δ
Langfjordjøkelen	10	-1.16	0.08	0.12	0.01	-1.39	0.13	0.08	-0.04	0.01	0.19

B glac. is mean annual glaciological mass balance
σ.glac. point is random error for each point value in the glaciological mass balance
σ.glac. spatial is spatial random error in the glaciological mass balance
σ.glac.ref is random error as a consequence of glacier area changes over time
B geod. is mean annual geodetic mass balance
σ.geod. DTM is random error for the DTMs
σ.dc is random error for the density conversion
B int is internal melting
σ.B. int is random error for the internal melting
Δ is the difference between glaciological and geodetic balance, corrected for internal melting

In order to check whether the annual discrepancy between glaciological and geodetic mass balance is significant different or not, a hypothesis where the uncertainties are taken into account, is tested (Zemp et al., 2013). If the answer of this hypothesis is «no», it is recommended to calibrate the glaciological mass balance series. If the answer is «yes», it means that the glaciological balance is not significant different from the geodetic balance. By checking this hypothesis for Langfjordjøkelen, the answer was «no», which means that the glaciological balance = the geodetic balance (Tab. 7). Hence, calibration of the series was not required.

Table 7
Comparison and check of glaciological and geodetic mass balance including the uncertainties.

Glacier	Δ	σ	H0	β	ε
Langfjordjøkelen	0.19	1.73	yes	59	0.39

Δ is the discrepancy (m w.e. a^{-1}) between glaciological and geodetic balance adjusted for internal melting
σ (dimensionless) is the reduced discrepancy, where uncertainties are accounted
H0 is the hypothesis whether the glaciological balance = the geodetic balance
β is the probability of accepting **H0** although the results of both methods are different at the 95 % confidence level
ε (m w.e. a^{-1}) is the limit for detection of bias

5 Conclusions

The aim of this report was to homogenize the glaciological mass balance series, compare the series with the geodetic mass balance, and hence, reveal a possibly significant discrepancy followed by a calibration of the glaciological series. The glaciological mass balance series covers the period from 1989 to 2018. Within this period, usable Digital Terrain Models (DTMs) from 1994, 2008 and 2018 were produced. In this report glaciological and geodetic mass balance were compared for the period 2008-2018.

In order to obtain comparable values the glaciological and the geodetic mass balances were first adjusted and homogenized. The homogenized cumulative glaciological mass balance series over the years 2009-2018 was −11.58 m w.e. The corresponding geodetic mass balance was −13.86 m w.e. The internal mass balance was quantified as −0.04 m w.e. a^{-1}. Accordingly, the mean annual difference ($\Delta_a = B_{a\ glac.} - B_{a\ geod.} + B_{a\ int.}$) over 2009-2018 was 0.19 m w.e. A hypothesis in Zemp et al. (2013) was tested and revealed that a calibration was not required.

The reanalysed mass balance values were updated in NVE's databases by flagging the series as homogenized. The annual mass balance data are available for download from NVE's glacier application http://glacier.nve.no/glacier/viewer/ci/en/. The reanalysed data will be submitted to WGMS.

References

Alexander, D., J. Shulmeister and T. Davies
2011: High basal melting rates within high-precipitation temperate glaciers. *Journal of Glaciology, Vol. 57, No. 205,* p. 789–795.

Andreassen, L.M., H. Elvehøy, B. Kjøllmoen and R. Engeset
2016: Reanalysis of long-term series of glaciological and geodetic mass balance for 10 Norwegian glaciers. *The Cryosphere, 10*, p. 535-552.

Andreassen, L.M., B. Kjøllmoen, A. Rasmussen, K. Melvold and Ø. Nordli
2012: Langfjordjøkelen, a rapidly shrinking glacier in northern Norway. *Journal of Glaciology, Vol. 58, No. 209,* p. 581–593.

Andreassen, L.M., H. Elvehøy, B. Kjøllmoen, R.V. Engeset, and N. Haakensen
2005: Glacier mass balance and length variation in Norway. *Annals of Glaciology, 42*, p. 317-325.

Andreassen, L.M.
1999: Comparing traditional mass balance measurements with long-term volume change extracted from topographic maps: A case study of Storbreen glacier in Jotunheimen, Norway, for the period 1940-1997. *Geografiska Annaler, 81 A (4)*, p. 467-476.

Bader, H.
1954: Sorge's Law of densification of snow on high polar glaciers. *Journal of Glaciology, 2(15),* p. 319–323.

Blom Geomatics AS
2008: LIDAR Rapport BNO07771 Langfjordjøkelen, 10 pp.

Cogley, J. G., R. Hock, A.L. Rasmussen, A.A. Arendt, A. Bauder, R.J. Braithwaite, P. Jansson, G. Kaser, M. Möller, L. Nicholson and M. Zemp
2011: Glossary of Glacier Mass Balance and Related Terms, *IHP-VII Technical Documents in Hydrology No. 86, IACS Contribution No. 2, Paris, UNESCO-IHP,* 114 pp.

Cuffey, K.M. and W.S.B. Paterson
2010: The Physics of Glaciers, 4th edition. Butterworth-Heinemann, Oxford, 704 pp.

Haug, T., C. Rolstad, H. Elvehøy, M. Jackson and I. Maalen-Johansen
2009: Geodetic mass balance of the western Svartisen ice cap, Norway, in the periods 1968-1985 and 1985-2002. *Annals of Glaciology 50 2009*, p. 191-197.

Huss, M.
2013: Density assumptions for converting geodetic glacier volume change to mass change. *The Cryosphere, 7, 877–887*, doi:10.5194/tc-7-877-2013.

Kjøllmoen, B. (Ed.), L.M. Andreassen, H. Elvehøy and M. Jackson
2018: Glaciological investigations in Norway 2017. *NVE Report 82 2018*, 84 pp.

Kjøllmoen, B. (Ed.)
2016: Glaciological investigations in Norway 2011-2015. *NVE Rapport 88 2016*, 171 pp.

Kjøllmoen, B and H.C. Olsen
2002: Langfjordjøkelen i Vest-Finnmark. Glasiohydrologiske undersøkelser. *NVE Dokument 4 2002*, 35 pp.

Oerlemans, J.
2013: A note on the water budget of temperate glaciers. *The Cryosphere 7*, p. 1557-1564.

Terratec AS
2018: Rapport for luftbåren laserskanning. Langfjordjøkelen, 14 pp.

Zemp, M., E. Thibert, M. Huss, D. Stumm, C. Rolstad Denby, C. Nuth, S.U. Nussbaumer, G. Moholdt, A. Mercer, C. Mayer, P.C. Joerg, P. Jansson, B. Hynek, A. Fischer, H. Escher-Vetter, H. Elvehøy and L.M. Andreassen
2013: Reanalysing glacier mass balance measurement series. *The Cryosphere 7*, p. 1227-1245.

Zemp, M.
2010: Reanalysis of multi-temporal aerial images of Storglaciären, Sweden (1959-99) – Part 2: Comparison of glaciological and volumetric mass balances. *The Cryosphere 4*, p. 345-357.

NVE

Norwegian water resources and energy directorate

MIDDELTHUNSGATE 29
POSTBOKS 5091 MAJORSTUEN
0301 OSLO
TELEFON: (+47) 22 95 95 95

www.nve.no